CrossMark

REVIEW

Facial asymmetry quantitative evaluation in oculoauriculovertebral spectrum

Renzo Manara[1] · Giovanni Schifano[2] · Davide Brotto[2] · Rodica Mardari[3] ·
Sara Ghiselli[2] · Antonio Gerunda[4] · Cristina Ghirotto[5] · Stefano Fusetti[5] ·
Katherine Piacentile[5] · Renato Scienza[4] · Mario Ermani[2] · Alessandro Martini[2]

Abstract

Objectives Facial asymmetries in oculoauriculovertebral spectrum (OAVS) patients might require surgical corrections that are mostly based on qualitative approach and surgeon's experience. The present study aimed to develop a quantitative 3D CT imaging-based procedure suitable for maxillo-facial surgery planning in OAVS patients.

Materials and methods Thirteen OAVS patients (mean age 3.5 ± 4.0 years; range 0.2–14.2, 6 females) and 13 controls (mean age 7.1 ± 5.3 years; range 0.6–15.7, 5 females) who underwent head CT examination were retrospectively enrolled. Eight bilateral anatomical facial landmarks were defined on 3D CT images (porion, orbitale, most anterior point of frontozygomatic suture, most superior point of temporozygomatic suture, most posterior-lateral point of the maxilla, gonion, condylion, mental foramen) and distance from orthogonal planes (in millimeters) was used to evaluate the asymmetry on each axis and to calculate a global asymmetry index of each anatomical landmark. Mean asymmetry values and relative confidence intervals were obtained from the control group.

Results OAVS patients showed 2.5 ± 1.8 landmarks above the confidence interval while considering the global asymmetry values; 12 patients (92 %) showed at least one pathologically

✉ Renzo Manara
   rmanara@unisa.it

   Giovanni Schifano
   schifanognn@gmail.com

   Davide Brotto
   davidebrotto@hotmail.it

   Rodica Mardari
   rodica.mardari@sanita.padova.it

   Sara Ghiselli
   saraghiselli@alice.it

   Antonio Gerunda
   antonio.gerunda@sanita.padova.it

   Cristina Ghirotto
   cristina.ghirotto@sanita.padova.it

   Stefano Fusetti
   stefano.fusetti@unipd.it

   Katherine Piacentile
   kpiacentile@hotmail.com

   Renato Scienza
   renato.scienza@sanita.padova.it

   Mario Ermani
   mario.ermani@unipd.it

   Alessandro Martini
   alessandromartini@unipd.it

[1] Neuroradiologic Unit, Sezione di Neuroscienze, University of Salerno, Via S Allende 1, 89081 Salerno, Italy

[2] Department of Neurosciences, University of Padova, Padua, Italy

[3] Department of Neuroradiology, University Hospital of Padova, Padua, Italy

[4] Department of Neurosurgery, University Hospital of Padova, Padua, Italy

[5] Department of Maxillo-Facial Surgery, University Hospital of Padova, Padua, Italy

asymmetric landmark. Considering each axis, the mean number of pathologically asymmetric landmarks increased to 5.5 ± 2.6 (p = 0.002) and all patients presented at least one significant landmark asymmetry.

Conclusions Modern CT-based 3D reconstructions allow accurate assessment of facial bone asymmetries in patients affected by OAVS. The evaluation as a global score and in different orthogonal axes provides precise quantitative data suitable for maxillo-facial surgical planning.

Clinical relevance CT-based 3D reconstruction might allow a quantitative approach for planning and following-up maxillo-facial surgery in OAVS patients.

Keywords Oculoauriculovertebral spectrum · Goldenhar syndrome · Facial asymmetry · Computed tomography · Image reconstruction

Introduction

Oculoauriculovertebral spectrum (OAVS, OMIM 164210) [1] is a rare congenital condition (incidence 1:3500–5600 live births) [2–4] characterized by variable underdevelopment of facial structures originating from the first and second pharyngeal arches on one (85 % of cases) or both sides [3, 5]. The disease mostly results in jaw abnormalities with consequent hemifacial microsomia and facial asymmetry. The most severe cases present also with eye or spine involvement and are known as Goldenhar syndrome.

Craniofacial anomalies include mandibular, zygomatic, and maxillary bone and soft tissue structure abnormalities that might affect breathing, swallowing, and ability to speak and variably impair esthetic appearance. In addition, jaw ankylosis and malocclusion can affect masticatory function [6].

Surgical correction can restore facial symmetry and masticatory performance. Treatment plans must be tailored to each patient. Surgical planning is mostly based on surgeon experience but might be improved by current imaging techniques [7]. "Cephalometric radiography," based on plain radiographs, has been used since 1930. Since the introduction of CT and dedicated software, 3D reconstructions have been suggested as a valuable tool for planning and monitoring corrective surgery [8]. A highly accurate 3D assessment allows the surgeon to properly plan the surgical procedures. The quantitative data also enable the clinician to objectively evaluate the post treatment outcome. Hitherto, very few studies addressed this issue providing quantitative evaluation of facial asymmetry [9, 10], and no standardized approach is currently available. An asymmetry index obtained from the sum of the side-to-side differences with respect to the three reference orthogonal planes has been proposed. A global index should allow a better categorization of facial landmark asymmetry and improve the comparison of different populations but does not provide any information

about the asymmetry severity of facial landmark along each orthogonal axis. This information might be pivotal for tailoring the proper corrective surgery. We performed a CT study on OAVS patients proposing a score that, besides providing a global quantification of asymmetry, can also be decomposed according to the different orthogonal axes giving precise quantitative data suitable for maxillo-facial surgical planning.

Material and methods

Subjects

We retrospectively evaluated CT exams (whole head or maxillo-facial CT) of 13 patients (mean age 3.5 ± 4.0 years; 0.2–14.2, 6 females) affected from hemifacial microsomia and microtia (see Table 1). Eight patients also presented with ocular or vertebral abnormalities and fulfilled the criteria required for Goldenhar syndrome (mean age 3.5 ± 4.8 years; 0.2–14.2, 4 females). A whole head CT was available in 8/13 OAVS patients.

All subjects were outpatients referring to our Otolaryngology Department and were evaluated by a multidisciplinary team (maxillo-facial surgeon, ENT specialist, audiologist, geneticist, neuroradiologist).

Thirteen subjects (mean age 7.1 ± 5.3 years; 0.6–15.7, 5 females) who underwent head CT for reasons different from facial asymmetry (extracranial malignancy, spinal muscular atrophy, respiratory fungal infection, histiocytosis, polytrauma) represented our control group.

CT data acquisition and image processing

CT scans were acquired with different scanners (21/26 with Brilliance 6, Philips, Best, The Netherlands; 2/26 with Somatom Sensation Cardiac 64, Siemens, Forchheim, Germany; 2/26 with Brilliance 64, Philips, Best, The Netherlands; 1/26 with HiSpeed, GE Healthcare, Waukesha, WI, USA). Due to different scanners used, the CT acquisition protocol varied significantly in terms of mAs (median 160 mAs, range 51–500), KVp (median 120, range 90–140 KVp), and slice thickness (median 1 mm, range 0.75–2). A 512 × 512 matrix was used in all acquisitions; the field of view range was 128–348 mm (median 200 mm) with reconstruction voxel range 0.18–0.68 mm (median 0.39 mm). The CTs were acquired in axial plane with spiral/helical scan; coronal and sagittal multiplanar reconstructions were available but not used in this study. All exams (axial images) were transferred from our PACS to a workstation (Planning Station 6.0, BrainLAB®) and processed with iPlan® software (Stereotaxy and CMF).

In particular, axial images were reconstructed with surface rendering techniques by optimizing the Hounsfield unit value for the best representation of the bone structures according to

Table 1 The main clinical findings of the oculoauriculovertebral spectrum group

Patient	#01	#02	#03	#04	#05	#06	#07	#08	#09	#10	#11	#12	#13
Sex	F	M	F	F	F	M	M	M	F	M	F	M	M
Age (years)	3.2	0.5	1.6	2.2	0.7	0.2	6.2	1.8	14.2	6.6	0.5	1.2	6.3
Side	R	B	R	R	L	L	R	L	R	R	B	R	R
Aural atresia	+	+	+	+	+	+	+	+	+	+	+	+	+
Hemifacial microsomia	+	+	+	+	+	+	+	+	+	+	+	+	+
Vertebral abnormalities	–	+	–	–	+	+	–	+	+	+	+	–	–
Eye abnormalities	+	+	–	–	–	–	–	–	+	+	–	–	–

Shadowed columns are Goldenhar syndrome patients, i.e., beside hemifacial microsomia and aural atresia, ocular or vertebral anomalies were present

F female , M male , R right , L left , B bilateral,(+) presence, (–) absence

the age of the patient. The midsagittal plane was defined by specific anatomical landmarks, namely the nasion (Na) identified by the midpoint of the frontonasal suture, the bregma (Br) identified by the crossing of the coronal and sagittal sutures on top of the skull, the opisthion (Op) identified by the posterior midsagittal point on the posterior margin of the foramen magnum. Whenever the Br was not reliably identifiable (e.g., in newborns) the interincisal point (iip) was used. The transverse plane was considered as the plane orthogonal to the sagittal plane oriented according to the Frankfurt horizontal plane, i.e., from the most superior point of the external acoustic meatus (porion, Po) to the most inferior point of the infraorbital rim (orbitale, Or). In patients with asymmetry of the abovementioned points (Po and Or) in the z-axis, the midpoint of the left and right points was adopted for identifying the axial plane. The coronal plane was considered as the orthogonal plane with respect to the midsagittal and axial planes, passing through the Po. Table 2 reports all points considered useful by our maxillo-facial surgeons while evaluating facial asymmetry severity. After defining the reference planes and after positioning manually the landmarks, the software provided the distance in millimeter of the abovementioned points from the three planes. The side-to-side difference of the three measures in the orthogonal planes represented the landmark asymmetry. The global asymmetry was calculated according to the following formula [9]:

$$\text{Global asymmetry} = \sqrt{(Rdx - Ldx)^2 + (Rdy - Ldy)^2 + (Rdz - Ldz)^2}$$

with dx, dy, and dz, being the distance of any one point from midsagittal, coronal, and axial planes respectively; R and L refer to the patient's right and left side.

The control group provided the reference values (mean and standard deviation, SD). Among our patients, severe landmark asymmetry was considered when the calculated global asymmetry of each landmark was above the confidence interval (mean of normal subjects +1.96 SD). Beside global asymmetry, asymmetries in the different axes were also considered.

Table 2 Anatomical landmarks

Landmarks		Definition
Br	Bregma	Crossing of the coronal and sagittal sutures on top of the skull
Na	Nasion	Midpoint of the frontonasal suture
Op	Opisthion	Posterior midsagittal point on the posterior margin of the foramen magnum
iip	Interincisal point	Most mesial point of the tip of the crown of each upper central incisor
Po[a]	Porion	Most superior point of the external acoustic meatus
Or[a]	Orbitale	Most inferior point of the infraorbital rim
FZ[a]	Frontozygomatic suture	Most medial and anterior point of the frontozygomatic suture at the level of the lateral orbital rim
TZ[a]	Temporozygomatic suture	Most superior and anterior point of the temporozygomatic suture
Masc[a]	Maxilla	Most postero-lateral point of the maxilla
Go[a]	Gonion	The point at mandibular angle that is defined by dropping a perpendicular from the intersection point of the tangent lines to the posterior margin of the mandibular vertical ramus and inferior margin of the mandibular body or horizontal ramus
Cd[a]	Condylion	Most lateral point of the condylar head
FM[a]	Mental foramen	Central point of the mental foramen

[a] Bilateral landmark points

Moreover, after defining the midsagittal plane (see above) with iPlan CMF®, the left hemifacial bone structures were mirrored and superimposed to the right side bone structures and represented with multiplanar reconstruction and surface rendering technique, thus providing a visual though measurable representation of the head bone asymmetry.

Statistical analysis

All measures were compared between patients and controls by means of Student's *t* test when data were normally distributed or Mann-Whitney *U* test, when the considered landmark measures were not normally distributed or included less than 10 cases per group. The Kolmogorov-Smirnov test was applied to verify the normality of data.

All the previously defined procedures were carried out by two independent observers. Intra- and interrater reliability was then evaluated. For intrarater reliability, the landmarks during image processing were evaluated by re-measuring after a 2-week interval the asymmetry data for 22 subjects randomly chosen among patients and controls. For interrater reliability, the same 22 subjects were evaluated by a second observer. In addition, the absolute difference (in mm) between first and second measures was calculated. Reliability was tested by using the Pearson's *r*. The covariance analysis was performed testing the significance of dependence between test and retest values of the anatomical measures, considering as dependent variable the second sample and as independent variable the first sample. Significance was set at *p* < 0.05.

Results

Compared to controls, OAVS patients showed significant differences in the global score for the Or, Masc, FZ, TZ, Cd, Go, and FM landmarks. Considering each of the three orthogonal axes, significant asymmetry was observed for Or, Cd, and FM in the X plane; for FZ, TZ, and Go in the Y plane; and for Masc and Cd in the Z plane (see Table 3).

Twelve patients (92 %) showed global asymmetry values above the confidence interval for at least one landmark. Considering each orthogonal axis, 11/13, 10/13, and 11/13 patients showed abnormal asymmetry values with respect to the X, Y, and Z planes, respectively. All patients presented at least with one asymmetric landmark in at least one axis.

Asymmetries of all single patients affected by the OAVS are plotted in the electronic supplementary material; in particular, global asymmetry and asymmetry with respect to the three orthogonal axes are represented in the corresponding diagrams that also show normal references calculated in our control group (Online Resource 1). The diagrams and the table (Online Resource 2) report the asymmetry in millimeter, thus

**Table 3** Comparison of asymmetry of anatomical points for control and oculoauriculovertebral spectrum group

Landmarks	Control group		OAVS group		*p*
	Mean	SD	Mean	SD	
Global asymmetry					
Or	1.24	0.45	2.06	1.17	0.03
Masc	1.92	0.79	4.45	2.89	0.01
FZ	2.20	0.78	3.51	1.47	0.01
Po	1.52	1.24	1.16	0.57	0.78[a]
TZ	2.12	0.97	4.01	1.99	0.01
Cd	3.25	1.33	7.74	5.34	0.01
Go	3.76	2.08	6.75	2.67	0.01
FM	4.14	2.97	11.02	7.62	0.05[a]
X plane asymmetry					
Or	0.65	0.39	1.44	1.14	0.03
Masc	0.94	0.45	1.73	1.86	0.15
FZ	0.90	0.50	0.89	0.96	0.98
Po	1.34	1.26	1.06	0.64	0.87[a]
TZ	1.10	0.79	1.73	1.05	0.10
Cd	1.30	0.81	2.89	2.50	0.04
Go	2.50	2.04	1.86	2.37	0.53
FM	3.08	3.00	8.66	7.04	0.02[a]
Y plane asymmetry					
Or	0.84	0.41	1.10	0.90	0.35
Masc	0.88	0.91	2.36	1.42	<0.001
FZ	1.32	0.75	2.47	1.66	0.03
Po	0.37	0.28	0.16	0.14	0.13[a]
TZ	1.23	0.81	2.69	2.31	0.04
Cd	1.95	1.25	4.11	5.61	0.19
Go	1.02	0.60	3.60	2.71	0.01
FM	1.47	0.90	2.41	2.23	0.83[a]
Z plane asymmetry					
Or	0.34	0.23	0.40	0.41	0.66
Masc	0.94	0.76	2.83	2.52	0.02
FZ	1.11	0.77	1.72	1.09	0.12
Po	0.21	0.15	0.30	0.21	0.53[a]
TZ	0.92	0.59	1.53	1.15	0.10
Cd	1.72	1.05	4.31	2.86	0.01
Go	2.23	1.27	4.07	2.83	0.08
FM	1.57	1.43	4.65	5.21	0.42[a]

OAVS oculoauriculovertebral spectrum, *SD* standard deviation

[a] The Mann-Whitney (*U* test) was used; in all other cases, the Student's *t* test was applied

providing the surgeon a measure of the correction needed to re-establish facial symmetry.

To note, global asymmetry seems to be more sensitive when considering the whole group, but in each patient, the single-axis evaluation revealed more frequently significant asymmetries. In fact, in our cohort 2.5 ± 1.8 landmarks were
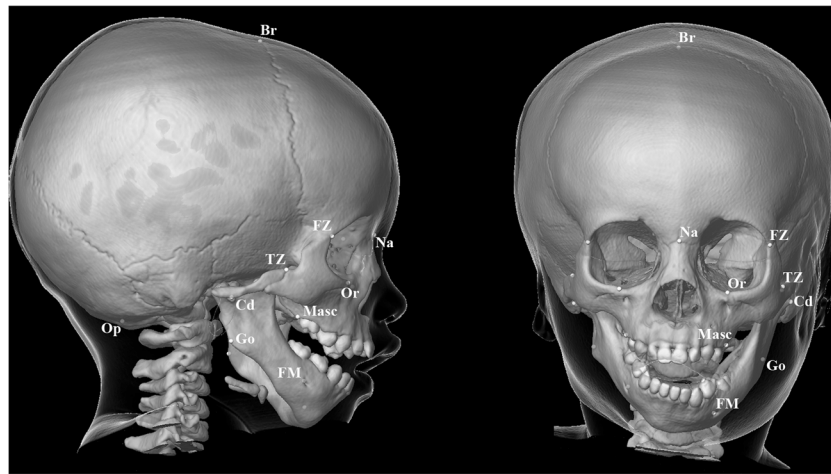
Fig. 1 Bone and skin surface rendering technique of patient #04 (right lateral and frontal view). All the landmarks used in the current study are reported except the porion, since the patient presented with right aural atresia; for this reason, asymmetry of this landmark was not calculable in most patients. *Br* bregma, *Na* nasion, *Op* opisthion, *iip* interincisal point, *Or* orbitale, *FZ* frontozygomatic suture, *TZ* temporozygomatic suture, *Masc* maxilla, *Go* gonion, *Cd* condylion, *FM* mental foramen

found above the confidence interval (mean value +1.96 SD obtained from controls) when considering the global asymmetry. Considering the asymmetry in all axes, the number of pathologic landmarks increased significantly to 5.5 ± 2.6 ($p = 0.002$).

The midsagittal plane was also used for mirroring the healthy or less affected side to the contralateral side in order to represent the severity of asymmetry of the bone segments.

Figures 1, 2, and 3 show surface rendering technique and multiplanar reconstructions in the three orthogonal planes of a patient: all these images are easily obtained and available for surgery planning.

Test and retest values and interrater measurements correlated very well ($r = 0.95$, $p < 0.000001$ and $r = 0.93$, $p < 0.000001$, respectively). Analysis of covariance showed no significant association between test and retest values and
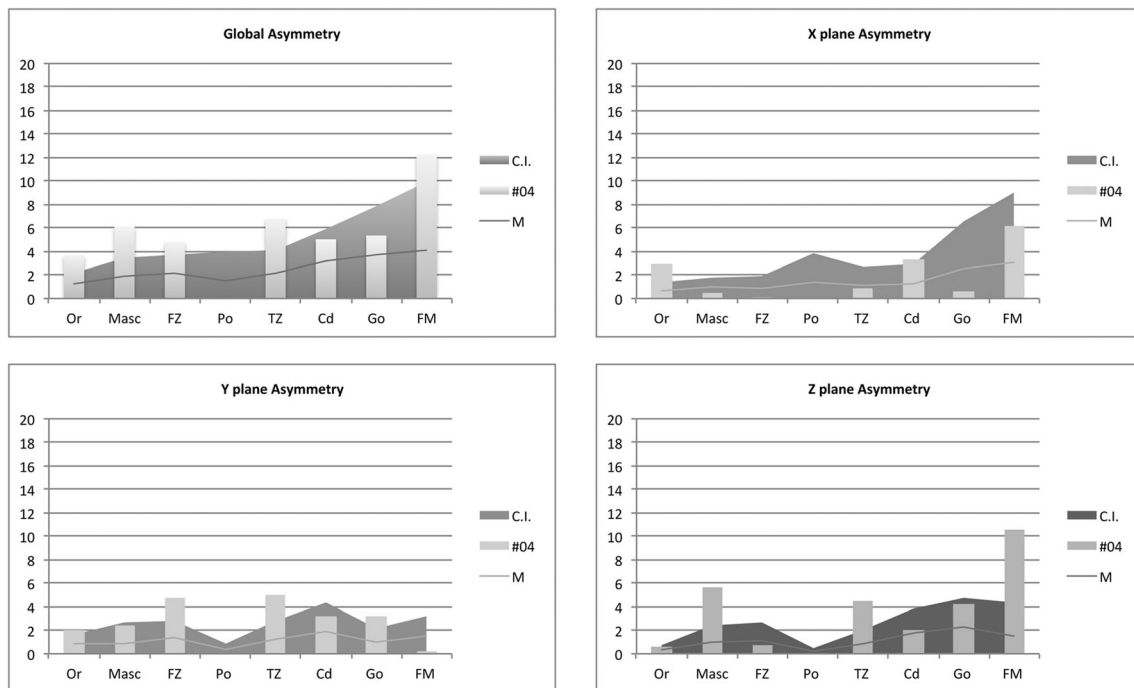
Fig. 2 Diagrammatic charts reporting the global and single (X, Y, Z) orthogonal plane asymmetry values of bone landmarks of patient #04. The *line and the upper limit of the shadowed area* represent the mean value (M) and the confidence interval (CI = M + 1.96 SD) of the normal values, respectively. The *bars* represent the patient's asymmetry value (see Online Resource 2). *Bars above the shadowed area* indicate significantly asymmetric landmarks
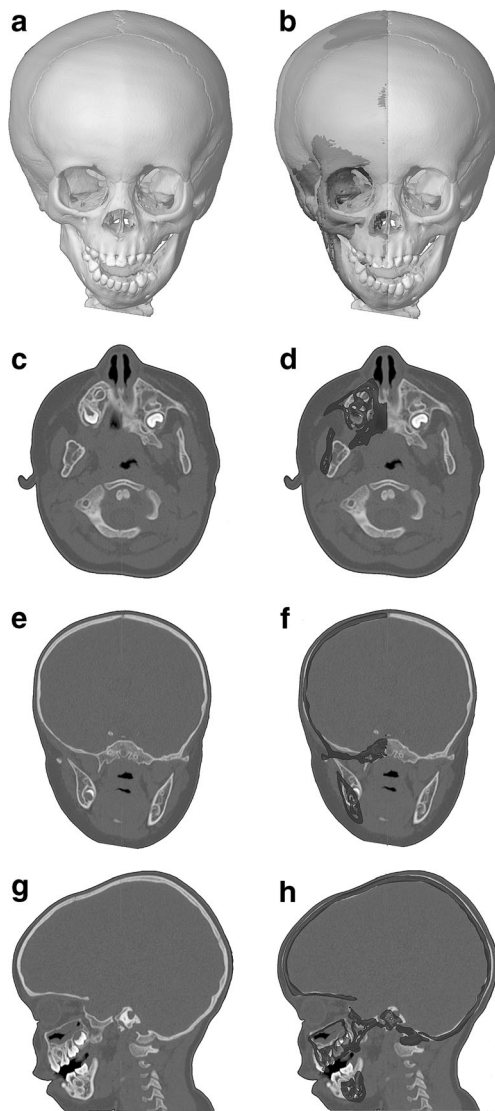
Fig. 3 CT-based reconstructions of patient #04 obtained to better show the bone structure asymmetry. The *left column* report the native images while in the *right column* the left hemiskull is mirrored on the right side. **a**, **b** Surface rendering technique, frontal view. **c–h** Multiplanar reconstruction images on axial (**c**, **d**), coronal (**e**, **f**), and sagittal (**g**, **h**) planes. In this patient, both maxilla and mandible are particularly affected

the anatomical measures. Mean absolute difference between first and second samples was 0.83 ± 0.78 mm (95 % CI 0.73–0.93). Mean absolute difference between rater was 0.68 ± 0.82 mm (95 % CI 0.62–0.75). For all landmarks, the mean absolute interobserver and intraobserver difference was <2 mm in all orthogonal planes.

Discussion

This study applied modern reconstruction techniques to investigate facial bone asymmetry in patients affected by hemifacial microsomia. Almost all OAVS patients showed global

asymmetry values above the confidence interval and all had abnormal asymmetry values when considering the orthogonal axes. According to this study, the evaluation in the three orthogonal axes showed to be more sensitive to asymmetry than the global score and likely provides more information on the correction required to re-establish the symmetry. In fact, the global score [9, 10] provides a measure of the asymmetry and it is useful to improve the characterization of a study cohort and allows population comparison across different studies. Nonetheless, the global score does not give any information on intervention needed to correct the asymmetry in the single patient. For this reason, single-axis asymmetry index should be provided in routine surgical planning.

A previous study compared an asymmetrical group (10 adult subjects with Menton deviation >4 mm from the facial midline) with a control group (11 adult subjects with Menton deviation <4 mm from the facial midline) among subjects who underwent whole head CT. The study showed a significantly increased asymmetry index of all the nine considered bone landmarks in the asymmetrical group [10]. We obtained a less optimal result most probably for two reasons: (1) the different approach used in the present study that did not subdivide the patients "a priori" according to the measured asymmetry and (2) the different age range with a prevalence of pediatric patients. The effect of age is particularly important when the asymmetry is provided as millimeter without taking into account the size of the head or bone structure. We preferred to provide row data (i.e. in mm) in order to assist the surgeon in planning the surgical correction instead of aiming to provide a tool for facial asymmetry diagnosis that is usually obtained by clinical observation. Indeed, the decision of surgical correction is based on esthetic reasons or masticatory impairment, while the CT examination should provide the surgeon with the measure needed to regain optimal facial symmetry. Besides providing a more precise characterization of facial asymmetry for surgery planning and follow-up, a quantitative approach would allow an improved comparison among OAVS populations and, therefore, an improved comparison in terms of surgical results. Some concern has emerged from the literature regarding the reproducibility of some landmark measurement [11]. In our study, all landmarks showed "high" (i.e., difference between observers <2 mm) or "very high" interobserver reproducibility (i.e., difference between observers <1 mm) supporting this method as reliable for surgical purposes.

A major problem of ours and previous studies using head CT evaluation was the definition of normative values. In fact, whole head exams in patients performing CT for a reason different from skull asymmetries are uncommon. Beside the abovementioned large age span of controls and patients, the relatively small number of controls likely explains the relatively large confidence interval found for the majority of landmarks. The enrolment of a higher number of controls, for

example, by sharing whole head CT scans obtained in different centers, will likely reduce the confidence interval and provide age classes-related values, thus improving the sensitivity and specificity of the asymmetry index. The usage of an index would be likely useful when evaluating the development of facial asymmetry along patient's growth to minimize the age interference, but focused studies are needed.

In addition, CTs performed under sedation often imply an incomplete mouth occlusion that might interfere with the symmetry evaluation of some landmarks on the mandible. Indeed, the latter might be partially displaced on one side altering the measurements of the relative landmarks, especially Go and FM as the condyle is fixed by the capsule and ligamentous elements of the temporomandibular joint. This might explain why FM and Go had the wider range among controls (see Fig. 2) and might reduce the reliability of this measurement when evaluating sedated OAVS patients. The retrospective design of our study did not allow to control the position of the mouth. Future studies will hopefully address these methodological aspects by controlling the position of the mandible during sedation.

As most of the patients are evaluated during childhood, the use of cone beam CT that administer a significantly lower radiation dose [12] should be preferred to conventional multislice CT. In fact, in spite of a higher resolution (the slice thickness can be less than 200 μm) cone beam CT radiation dose might be up to 90 below those of clinical multislice CT protocols [12]. The decreased ability of cone beam CT to investigate soft tissues compared to multislice CT should not be a problem in OAVS patients since a brain MRI is usually included in the diagnostic work-up. On the other hand, study limitations along the z-axis might limit cone beam CT to small children, when a whole head scan is required. In any case, the technique presented in this study can be easily applied also to images obtained with cone beam CT.

Conclusions

Craniofacial anomalies in oculoauriculovertebral spectrum patients might require surgical correction for restoring facial asymmetry and masticatory performance. So far, the approach for surgical planning was mostly based on surgeon's experience (qualitative approach). Modern CT-based 3D reconstructions represent an efficient tool for evaluating facial bone asymmetries in patients affected by oculoauriculovertebral spectrum. The evaluation both as a global score and in the different orthogonal axes provides precise quantitative data that are suitable for maxillo-facial surgical planning and follow-up. The collection of a large multicenter database of normative values is warranted to further improve the reliability of this technique. CT-based 3D reconstructions might allow a quantitative approach for the planning of maxillo-facial surgery in OAVS patients.

References

1. Online Mendelian Inheritance in Man, OMIM® (1995) [Updated 2015 Apr 29] McKusick-Nathans Institute of Genetic Medicine, Johns Hopkins University School of Medicine (Baltimore, MD) and National Center for Biotechnology Information (Baltimore, MD). http://omim.org Accessed 07 May 2015
2. Poswillo D (1974) Otomandibular deformity: pathogenesis as a guide to reconstruction. J Maxillofac Surg 2(2–3):64–72
3. Grabb WC (1965) The first and second branchial arch syndrome. Plast Reconstr Surg 36(5):485–508
4. Rollnick BR, Kaye CI, Nagatoshi K, Hauck W, et al. (1987) Oculoauriculovertebral dysplasia and variants: phenotypic characteristics of 294 patients. Am J Med Genet 26(2):361–375
5. Mastroiacovo P, Corchia C, Botto LD, et al. (1995) Epidemiology and genetics of microtia-anotia: a registry based study on over one million births. J Med Genet 32(6):453–457
6. Heike CL, Luquetti DV, Hing AV. (2009) [Updated 2014 Oct 09] Craniofacial microsomia overview. GeneReviews® http://www.ncbi.nlm.nih.gov/books/NBK5199. Accessed 07 May 2015
7. Saccomanno S, Greco F, D'Alatri L, De Corso E, Pandolfini M, Sergi B, Pirronti T, Deli R (2014) Role of 3D-CT for orthodontic and ENT evaluation in Goldenhar syndrome. Acta Otorhinolaryngol Ital 34(4): 283–287
8. Kawamata A, Ariji Y, Langlais RP (2000) Three-dimensional computed tomography imaging in dentistry. Dent Clin N Am 44(2):395–410
9. Katsumata A, Fujishita M, Maeda M, Ariji Y, Ariji E, Langlais RP (2005) 3D-CT evaluation of facial asymmetry. Oral Surg Oral Med Oral Pathol Oral Radiol Endod. 99(2):212–220
10. Yáñez-Vico RM, Iglesias-Linares A, Torres-Lagares D, Gutiérrez-Pérez JL, Solano-Reina E (2011) Three-dimensional evaluation of craniofacial asymmetry: an analysis using computed tomography. Clin Oral Investig 15(5):729–736
11. Olszewski R, Tanesy O, Cosnard G, Zech F, Reychler H (2010) Reproducibility of osseous landmarks used for computed tomography based three-dimensional cephalometric analyses. J Craniomaxillofac Surg 38(3):214–221
12. Loubele M, Bogaerts R, Van Dijck E, Pauwels R, Vanheusden S, Suetens P, Marchal G, Sanderink G, Jacobs R (2009) Comparison between effective radiation dose of CBCT and MSCT scanners for dentomaxillofacial applications. Eur J Radiol 71(3):461–468